한국해양공학회지 제19권 제5호, pp 1~15, 2005 (ISSN 1225-0767)

Motion Analysis of Two Floating Platforms with Mooring and Hawser Lines in Tandem Moored Operation by Combined Matrix Method and Separated Matrix Method

BON-JUN KOO* AND MOO-HYUN KIM**

*Basic Design Part, Offshore Design Team, Samsung Heavy Industries Co. Ltd, Geoje, Korea

**Coastal and Ocean Engineering Program, Department of Civil Engineering, Texas A&M University, College Station, USA.

KEY WORDS: Hull-mooring-riser Coupling, FPSO, Shuttle Tanker, Tandem Moored, Multiple Floating Bodies, Combined Matrix Method, Separated Matrix Method

ABSTRACT: *The motion behaviors including hydrodynamic interaction and mechanical coupling effects on multiple-body floating platforms are simulated by using a time domain hull/mooring/riser coupled dynamics analysis program. The objective of this study is to evaluate off-diagonal hydrodynamic interaction effects and mechanical coupling effects on tandem moored FPSO and shuttle taker motions. In the multiple-body floating platforms interaction, hydrodynamic coupling effects with waves and mechanical coupling effects through the connectors should be considered. Thus, in this study, the multiple-body platform motions are calculated by Combined Matrix Method (CMM) as well as Separated Matrix Method (SMM). The advantage of the combined matrix method is that it can include all the 6Nx6N full hydrodynamic and mechanical interaction effects among N bodies. Whereas, due to the larger matrix size, the calculation time of Combined Matrix Method (CMM) is longer than the Separated Matrix Method (SMM). On the other hand, Separated Matrix Method (SMM) cannot include the off-diagonal 6x6 hydrodynamic interaction coefficients although it can fully include mechanical interactions among N bodies. To evaluate hydrodynamic interaction and mechanical coupling effects, tandem moored FPSO and shuttle tanker is simulated by Combined Matrix Method (CMM) and Separated Matrix Method (SMM). The calculation results give a good agreement between Combined Matrix Method (CMM) and Separated Matrix Method (SMM). The results show that the Separated Matrix Method (SMM) is more efficient for tandem moored FPSO and shuttle tanker. In the numerical calculation, the hydrodynamic coefficients are calculated from a 3D diffraction/radiation panel program WAMIT, and wind and current forces are generated by using the respective coefficients given in the OCIMF data sheet.*

1. INTRODUCTION

As demands of oil and gas growth, the new concept of multiple-body floating platforms operations, such as FPSO and shuttle tanker operation or LNG terminal and LNG carrier operation, are preferred in deepwater oil and gas field. In the deepwater operation, FPSO or LNG terminal can store oil and gas in their storage tank. However, the FPSO or LNG terminal needs offloading operations. If multiple-body operation is available, offloading operation can be simpler and cheaper than install new underwater pipeline in remote deepwater oil and gas field. For offloading oil from FPSO, the distance and arrangement of multiple floating platforms are much flexible than offloading LNG. The reason is that the offloading the liquefied gas, the flow lines overcome extremely low temperature, thus, in LNG offloading operation, the arrangement and the distance between LNG terminal and LNG carrier are restricted by LNG off-loading lines.

The hydrodynamic interactions between multiple bodies have been reported by many researchers; Ohkushu (1974), Kodan (1984), Fang and Kim (1986) analyze the hydrodynamic interaction by using strip theory, Vanm Oortmerssen (1979) and Loken (1981) used the three dimensional linear diffraction theory, and Choi and Hong (2002) used three dimensional higher order diffraction theory. Whereas, the time domain multiple bodies interaction is studied recently by Buchner et al. (2001), Hong et al.

제1저자 구본준 연락처: 경상남도 거제시 상동리 479

055-638-2458 seanku@hanmail.net

(2003), Lee (2002), and Kim (2003). Buchner et al. (2001), Lee (2002), and Kim (2003) calculate hydrodynamic coefficients from three dimensional linear diffraction theories and convert these coefficients into time domain to calculate the multiple-body motion, and Hong et al. (2003) also do same manner except using higher order diffraction theories.

To evaluate realistic motion responses of multiple floating platforms, there are additional aspects to be considered. The first aspect is mechanical coupling between multiple-body platforms. The multiple floating bodies have many slender members, such as mooring lines, risers, and hawsers. The dynamic interactions between hull and slender members can be evaluated by numerically in several ways. One simple approach is called uncoupled analysis, which assumed that mooring lines, risers, and hawsers respond statically (as massless nonlinear spring) to hull motion (eg. Lee (2002)). With this assumption, the inertia effects and hydrodynamic loading on the slender members are neglected. Thus, in uncoupled analysis, mooring dynamic can be evaluated after calculating hull motion and input the hull fairlead motions.

The reliability and accuracy of this approach can be diminished as water depth increase. Kim et al. (2001a and 2001b), and Ma et al. (2000) showed that such uncoupled analysis of TLPs and spars may be inaccurate when used in deepwater. Wichers et al. (2001a and 2001b) showed that uncoupled analysis may give even larger error in case of weathervane FPSO or FPSO/LNG. Wichers et al (2001a and 2001b) concluded that fully coupled dynamic models are prerequisite to estimate realistic design values. The second aspect is that most of FPSOs are using weathervane turret-mooring system. To evaluate realistic response of tandem moored FPSO and shuttle tankers in wind, wave, and current, the large yaw motion should be considered. Several researchers have studied the dynamic characteristics of FPSO in wind, wave, and current. Whichers (1988) initiated a comprehensive study for numerical simulations of a turret-moored FPSO in irregular wave with wind and currents. Wichers (1988) derived the equation of motions of such model in the time domain using an uncoupled method. Other researchers (eg. Sphier et al. (2000), Lee and Choi (2000)) investigated the behavior and stability of turret-moored FPSOs based on a set of simplified methods.

The time domain hull /mooring /riser coupled analysis of turret moored FPSO was carried out by 3-D hull/mooring/riser coupled dynamics program, WINPOST, based on a CMM (Arcandra (2002)). Kim (2003) extends Arcandra's works to multiple-body floating platforms which can consider full 6N×6N hydrodynamic interaction between multiple-body floating platforms. Kim (2003) used CMM which can consider the full hydrodynamic interactions and slender members coupling effects. Kim (2003) analyzed motion response of the tandem moored FPSO and shuttle tanker successfully. Another way to calculate multiple-body floating platform interaction is SMM. The SMM cannot include off-diagonal 6×6 hydrodynamic interaction between platforms, but this method can evaluate the mechanical coupling between multiple-body floating platforms. Using SMM, the matrix size can be reduced and this will reduce calculation time.

The main objective of this study is to evaluate hydrodynamic interactions and mechanical coupling effects on tandem moored FPSO and shuttle tanker. Thus, in this study, CMM and SMM are using for evaluating motion responses of tandem moored multiple floating bodies.

2. FORMULATION

2.1 Hydrodynamic of Multiple Floating Bodies in Time Domain Analysis

When a three-dimensional body interacts with incident wave in the fluid domain, the hydrodynamic coefficient and the wave exciting force and moment on large floating structure can be obtained by using three dimensional first- and second-order diffraction theory. In the diffraction theory, the total velocity potential can be decomposed by incident wave potential, diffraction potential, and radiation potential and the total velocity potential satisfy the Lapalce equation, bottom boundary condition, free surface boundary condition, body boundary condition, and Sommerfield radiation boundary condition. In general, single floating body platform motion can be described by 6 degrees of freedom motions. For multiple floating bodies system have 6 x number of body. In the diffraction boundary, multiple floating bodies can be modeled as single fixed body in the fluid domain. Thus, the diffraction problem can be expressed as follow;

$$\frac{\partial \phi_7^I}{\partial n} = -\frac{\partial \phi_I}{\partial n} \quad \text{on} \quad S_I \tag{1}$$

$$\frac{\partial \phi_7^{II}}{\partial n} = -\frac{\partial \phi_I}{\partial n} \quad \text{on} \quad S_{II} \tag{2}$$

where S_I and S_{II} denotes the wetted surface of the isolated body I and II respectively, ϕ_7^I and ϕ_7^{II} denotes the diffraction potential to the isolated body I and II respectively, and ϕ_I represents the incident wave potential of the isolated body.

The radiation potential for the isolated body can be

decomposed in the similar manner as single body problem.:

$$\phi_R^I = \sum_{j=1}^{6} \zeta_j \phi_j^I \tag{3}$$

$$\phi_R^{II} = \sum_{j=1}^{6} \zeta_j \phi_j^{II} \tag{4}$$

The radiation boundary for the isolated body *I* and *II* can be given by:

$$\frac{\partial \phi_j^I}{\partial n} = n_j^I \quad \text{on} \quad S_I \quad (j = 1, 2,...,6) \tag{5}$$

$$\frac{\partial \phi_j^{II}}{\partial n} = n_j^{II} \quad \text{on} \quad S_{II} \quad (j = 1, 2,...,6) \tag{6}$$

where ϕ_j^I and ϕ_j^{II} denotes the decomposed radiation potential components for the isolated body *I* and *II* respectively, and $n_j^{I,II}$ is a unit normal vector for the six degree of freedom for the isolated body *I* and *II* respectively. In equation (5) and (6), $n_j^{I,II}$ is given by:

$$n_j^{I,II} = \begin{cases} (n_1, n_2, n_3)^{I,II} & \text{for } j = 1,2,3 \\ (n_4, n_5, n_6)^{I,II} = \tilde{\mathrm{r}} \times \mathrm{n}^{\mathrm{I,II}} & \text{for } j = 4,5,6 \end{cases} \tag{7}$$

where $\tilde{\mathrm{r}}$ denotes the relative distance from the origin to each body center.

The boundary-value equation and the boundary condition for interaction problem for each body can be defined as the form of the radiation/scatter potential. The following equations express the interaction problems on both bodies.

Interaction problem -radiation/diffraction for 1st body near 2nd body:

$$\frac{\partial \widehat{\phi}_j^I}{\partial n} = -\frac{\partial \phi_j^I}{\partial n} \quad \text{on} \quad S_I \quad (j = 1, 2,...,7) \tag{8}$$

$$\frac{\partial \widehat{\phi}_j^I}{\partial n} = 0 \quad \text{on} \quad S_{II} \quad (j = 1, 2,...,7) \tag{9}$$

Interaction problem -radiation/diffraction for 1st body near 2nd body:

$$\frac{\partial \widehat{\phi}_j^H}{\partial n} = -\frac{\partial \phi_j^{II}}{\partial n} \quad \text{on} \quad S_{II} \quad (j = 1, 2,...,7) \tag{10}$$

$$\frac{\partial \widehat{\phi}_j^H}{\partial n} = 0 \quad \text{on} \quad S_I \quad (j = 1, 2,...,7) \tag{11}$$

where $\widehat{\phi}_j^{I,II}$ denotes the interaction potential affected by radiation/diffraction potential from the 1st body to the 2nd body, and vice versa. The potential when $j = 7$ means the diffraction term.

In this study, the hydrodynamic coefficients, such as added mass, radiation damping, first- and second-order mean and difference frequency forces were calculated from the three-dimensional second-order diffraction/radiation panel program WAMIT (Lee, 1999). To convert the frequency domain hydrodynamic coefficients into time domain, the force coefficients are expressed as a two-term Volttera series expression, and the frequency-dependent radiation damping is included in the form of convolution integral.

To calculate the motion responses of multiple floating bodies, the equation of motion can be expressed as following matrix;

$$\begin{bmatrix} M_1 + m_{1,1}^a(\infty) & \cdots & m_{1,N}^a(\infty) \\ \vdots & \ddots & \vdots \\ m_{N,1}^a(\infty) & \cdots & M_N + m_{N,N}^a(\infty) \end{bmatrix} \begin{pmatrix} \ddot{x}_1 \\ \vdots \\ \ddot{x}_N \end{pmatrix} + \begin{bmatrix} \int R_{1,1}(t-\tau)d\tau & \cdots & \int R_{1,N}(t-\tau)d\tau \\ \vdots & \ddots & \vdots \\ \int R_{N,1}(t-\tau)d\tau & \cdots & \int R_{N,N}(t-\tau)d\tau \end{bmatrix} \begin{pmatrix} \dot{x}_1 \\ \vdots \\ \dot{x}_N \end{pmatrix} + \begin{bmatrix} K_{1,1} & \cdots & \\ \vdots & \ddots & \\ \cdots & & K_{N,N} \end{bmatrix} \begin{pmatrix} x_1 \\ \vdots \\ x_N \end{pmatrix} = \begin{pmatrix} F_1 \\ \vdots \\ F_N \end{pmatrix} \tag{12}$$

where, M is 6x6 structure mass matrix, m is added mass matrix at infinite frequency, R is the retardation function matrix, K is the hydrostatic restoring coefficient matrix, x is motion vector, and F is external force vector. The subscript represents the body number. The force vector includes wave exciting force, wind force, current force, and wave drift force. In the numerical simulation, the wave drift damping is calculated by Aranhas formula and the effects are found to be small (Arcandra, 2001), thus wave drift damping is not considered in this study. The second-order wave exciting

forces are approximated by Newmans approximation. The Newmans approximation can be justified when the systems natural frequency is very small and the slope of quadratic force transfer function near the diagonal is not large. In Kim (2003) the validity of Newmans approximation is tested and the results were reasonable compare with more accurate results with complete quadratic force transfer function.

2.2 Mechanical Coupling between Multiple Floating Bodies and Slender Members

In a time domain coupled dynamic analysis, the mooring, riser and platform dynamics are solved simultaneously as an integrated system. In the analysis, the hydrodynamic force on the platform are evaluated by 3 dimensional diffraction theory. The first-order wave forces, added mass and radiation damping, and the second-order mean and difference frequency forces on the platform are evaluated by WAMIT (Lee, 1999). The sum-frequency parts are not important for spar platform, thus not included in the motion analysis. The wave force linear and quadratic transfer functions (LTF and QTF) are calculated in the frequency domain, and then these forces are converted to the time domain using the two-term Volterra series expansion. The frequency dependent radiation damping is included in the form of a convolution integral in the time domain simulation.

For the static/dynamic analysis of the mooring and riser system, an extension of the theory developed for the dynamics of slender rods by Garrett (1982) is used in WINPOST. A brief summary of slender finite element formulation for a slender rod follows. Assuming no torque or applied external twisting moment, one can derive the linear momentum conservation equation with respect to a position vector $\vec{r}(s,t)$ that is a function of arc length *(s)* and time *(t)*:

$$-(B\vec{r}'')'' + (\lambda\vec{r}')' + \vec{q} = m\ddot{\vec{r}} \tag{13}$$

$$\lambda = T - B\varkappa^2 \tag{14}$$

$$T = T_0 + P_e A_e - P_i A_i \tag{15}$$

where, prime and dot denotes spatial and time derivative, respectively, B is bending stiffness, T, the local effective tension, $\varkappa$, the local curvature, m, the mass per unit length, $\vec{q}$, the distributed force on the rod per unit length, T_0, the local tension, P_e, the external pressures, P_i, the internal pressures, A_e and A_i are external and internal cross-sectional areas. The scalar variable λ can be regarded as a Largrange multiplier. If the rod is assumed to be in extensible, the following condition must be satisfied:

$$\vec{r}' \cdot \vec{r}' - 1 = 0 \tag{16}$$

If the rod is extensible, the following relation can be used

$$\frac{1}{2}(\vec{r}' \cdot \vec{r}' - 1) = \frac{T}{EA_t} \approx \frac{\lambda}{EA_t} \tag{17}$$

$$A_t = A_e - A_i \tag{18}$$

For these equations, the geometric nonlinearity is fully considered there is no special assumption made concerning the shape or orientation of the mooring lines, as long as the rod remains elastic. The normal component of the distributed external force on the rod per unit length, q_n, is given by the generalized Morison equation

$$q_n = C_I \rho A_e \dot{v}_n + \frac{1}{2} C_D \rho D |v_{nr}| v_{nr} + C_m \rho A_e \ddot{r}_n \tag{19}$$

where C_I, C_D, and C_m are inertia, drag and added mass coefficients, and $\dot{v}_n$, v_{nr}, and $\ddot{r}_n$ are normal fluid acceleration, normal relative velocity, and normal structure acceleration, respectively. The symbols ρ and D are fluid density and local diameter. in addition, the effective weight, or net buoyancy, of the rod should be included in q_n, as a static load. To develop the finite element formulation, consider a single element of length L, and use the following expression:

$$\vec{r}(s,t) = \sum_i A_i(s)\vec{U}_i(t) \tag{20}$$

$$\lambda(s,t) = \sum_m P_m(s)\lambda_m(t) \tag{21}$$

where A_i and P_m are Hermitian cubic and quadratic interpolation functions defined on the interval $o \le s \le L$. Using equation (20) and (21), equation (13) can be reduced to the following equation by the Galerkins method and integration by parts (Garrett, 1982):

$$\int_0^L [B\vec{r}''A_i'' + \lambda\vec{r}'A_i' - \vec{q}A_i' + m\ddot{\vec{r}}A_i]ds$$
$$= B\vec{r}''A_i' \,|_0^L + \lambda\vec{r}' - (B\vec{r}'')'A_i \,|_0^L \tag{22}$$

where it is assumed that the shape function A_i continuous on the element. The first boundary term of the right-hand side is related to the moments on the ends, and the second term is the force on the ends, i.e. they are natural boundary conditions. If equation (16) is used, we obtain:

$$\int_0^L P_m\left\{\frac{1}{2}(\vec{r}'\vec{r}'-1)-\frac{\lambda}{EA_i}\right\}ds=0 \tag{23}$$

The position vector, its tangent, and the Lagrange multiplier are selected to be continuous at a node between adjacent element.

Elements are combined using the continuity of $\vec{r}$, $\vec{r}'$, and λ. The natural boundary conditions at joint cancel out, leaving those conditions applicable at the ends of the rod. The upper ends of these risers and mooring lines are connected to the hull through a generalized translational and rotational spring that can also model both fixed and hinged boundary conditions at its limit. The forces and moments proportional to the relative displacements are transmitted to the hull at the connection points. The transmitted force from mooring lines and risers to the platform are given by:

$$F_p=K(Tu_p-u_I)+C(T\dot{u}_p-\dot{u}_I) \tag{24}$$

where K is the stiffness matrix, C, the damping matrix, T, the transformation matrix between the platform origin and connection point, u_p and u_I are displacement vectors of the platform and connection point.

The hull response equation is combined into the mooring line equation in the time-domain as follows::

$$\begin{aligned}&(M+M_a(\infty))\ddot{u}_p+\int_0^\infty R(t-\tau)\dot{u}_p d\tau+K_H u_p\\&=F_{(D)}+F^{(1)}+F^{(2)}+F_p+F_{WD}\end{aligned} \tag{25}$$

where, M and M_a are structure mass and added mass, R the retardation function (inverse cosine Fourier transform of radiation damping), K_H the hydrostatic restoring coefficients, F_D the drag force matrix on the hull, $F^{(1)}$, $F^{(2)}$ the first- and second-order wave load matrices on the hull, F_p the transmitted force matrix from the interface, and F_{WD} the wave drift damping force matrix. The added mass at infinite frequency is obtained from Kramers-Kroing relation. For the time series of $F^{(1)}$, $F^{(2)}$, and F_{WD} a two-term Volttera series is used. From above time-domain equation of motion, the hull/mooring line/riser coupled analysis can be achieved.

In the static analysis of mooring lines and risers, WINPOST uses the Newton's iteration methods. Thus, the coupled force on the mooring at $(n+1)^{th}$ iteration can be approximated by the rule at (n)th iteration.

$$N_i^{(n+1)}=N_i^{(n)}+\frac{\partial N_i}{\partial r_j}\triangle r_j+\frac{\partial N_i}{\partial X_j}\triangle X_j+\frac{\partial N_i}{\partial \theta_j}\triangle \theta_j \tag{26}$$

Similarly, the connection force on the platform at (n+1)th iteration can be approximated by:

$$F_i^{(n+1)}=F_i^{(n)}+\frac{\partial F_i}{\partial r_j}\triangle r_j+\frac{\partial F_i}{\partial X_j}\triangle X_j+\frac{\partial F_i}{\partial \theta_j}\triangle \theta_j \tag{27}$$

$$M_i^{(n+1)}=M_i^{(n)}+\frac{\partial M_i}{\partial r_j}\triangle r_j+\frac{\partial F_i}{\partial X_j}\triangle X_j+\frac{\partial M_i}{\partial \theta_j}\triangle \theta_j \tag{28}$$

Equation (26) shows that the mooring at connecting node is coupled with the unknown platform motion. The second term in the right hand side of equation (26), (27), and (28) are included in the equation of mooring element which is coupled with the platform and third and fourth terms in the equation (26), (27), and (28) are included in the equation of the platform. The mooring and platform are coupled by the third and fourth terms in the equation (26) and the second terms in the equation (27) and (28). The connection force vectors $N_i^{(n)}$, $F_i^{(n)}$, and $M_i^{(n)}$, are added to the force vectors at the right side of the equations of the mooring element and platform. At each iteration, the coupled algebraic equations are solved to obtain the solutions simultaneously. The iteration continues until a specific tolerance is reached.

In the time domain integration, the coupled force on the mooring is added to the equation of platform motion and is integrated from time $t^{(n)}$ to $t^{(n+1)}$t$^{(n+1)}$:

$$\begin{aligned}\int_{t^{(n)}}^{t^{(n+1)}} N_i dt&=\frac{\triangle t}{2}(N_i^{(n+1)}+N_i^{(n)})\\&\approx\frac{\triangle t}{2}\left(N_i^{(n)}+\frac{\partial N_i}{\partial r_j}\triangle r_j+\frac{\partial N_i}{\partial X_j}\triangle X_j+\frac{\partial N_i}{\partial \theta_j}\triangle \theta_j+2N_i^{(n)}\right)\end{aligned} \tag{29}$$

$$\int_{t^{(n)}}^{t^{(n+1)}} F_i dt = \frac{\triangle t}{2}\left(F_i^{(n+1)} + F_i^{(n)}\right)$$
$$\approx \frac{\triangle t}{2}\left(F_i^{(n)} + \frac{\partial F_i}{\partial r_j}\triangle r_j + \frac{\partial F_i}{\partial X_j}\triangle X_j + \frac{\partial F_i}{\partial \theta_j}\triangle \theta_j + 2F_i^{(n)}\right) \quad (29)$$

$$\int_{t^{(n)}}^{t^{(n+1)}} M_i dt = \frac{\triangle t}{2}\left(M_i^{(n+1)} + M_i^{(n)}\right)$$
$$\approx \frac{\triangle t}{2}\left(M_i^{(n)} + \frac{\partial M_i}{\partial r_j}\triangle r_j + \frac{\partial M_i}{\partial X_j}\triangle X_j + \frac{\partial M_i}{\partial \theta_j}\triangle \theta_j + 2M_i^{(n)}\right) \quad (30)$$

Like the static analysis, the coefficients in the above equations go to the time domain equations of the platform and the element of the mooring coupled with the platform.

The difference between single body and multiple bodies coupled analysis can be found in assembling the global matrix that includes the hydrodynamic coefficients and mechanical coupling coefficients of hull and slender members. In this study, two different methods are used in assembling the global matrix. The first method is CMM. In this method, all the hydrodynamic coefficients and mechanical coupling coefficients of hull and slender members are included in one large matrix. The second method is SMM. In this method, the global matrix is separated by each floating body and the mechanical coupling between two bodies is calculated by static tension force from hawser members. The hawser lines are generally in the air and the length of hawser lines are short compare to mooring lines and risers, thus the inertia effects and the drag force from the hawsers are expected to be very small. The major difference between CMM and SMM occurs in off-diagonal 6x6 added mass matrix and radiation damping matrix. Due to separate global matrix by each body, the SMM cannot consider the off-diagonal hydrodynamic interaction terms. The global matrix formulations are illustrated in following Fig. 1 and Fig. 2. In Fig. 1 and Fig. 2, sub-matrix K_M represents the coefficients for mooring line and riser, sub-matrix K_H represents the coefficient for hawser, sub-matrix K_{CMP} and K_{CH} represent coupling coefficient between hull and slender members, and sub-matrix K_P represents the coefficients for hull. The superscript in K_P matrix represents body number. The vectors U and F represent displacement and force of hull and slender members.

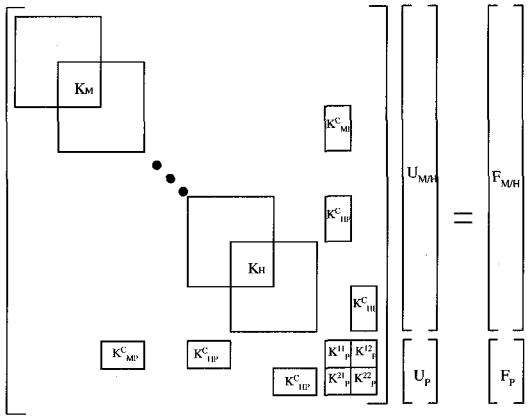

Fig. 1 Global matrix of combined matrix method (example for two bodies)

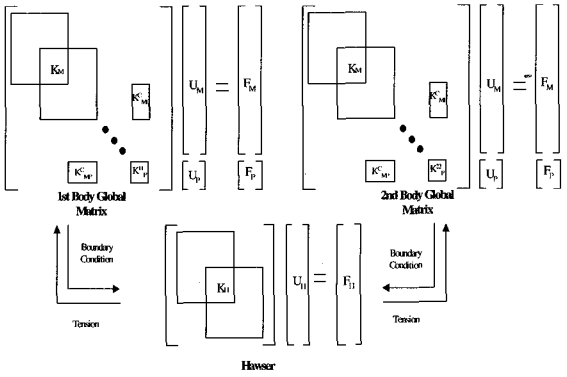

Fig. 2 Global matrix of separated matrix method (example for two bodies)

As illustrated in Fig. 1, the CMM includes the entire coefficient in one large matrix and inverse the global matrix in every time step. Fig. 2 shows that the SMM divides global matrix by each body and solve mechanical coupling by through hawser solving matrix. In the calculation, each body motions are given as essential boundary condition of hawser end point and the hawser tension is given to each body as external force. Due to the separation of global matrix, the off-diagonal 6x6 cannot be included in SMM (i.e. K_{12P} and K_{21P} in Fig. 1). Thus, the CMM is the most accurate way to calculate the multiple-floating-body interactions problem. However, in the CMM, the matrix size is large when the number of body and slender member increased. Due to large matrix size, the calculation time is much longer than SMM. The off-diagonal 6×6 hydrodynamic interaction effects are varies with the arrangement and the distance between multiple floating bodies. Thus, when hydrodynamic interaction effects are smaller than mechanical coupling

effects, the separation matrix method can be the efficient way to solve multiple floating platforms motion responses.

3. SPECIFICATION OF FPSO AND SHUTTLE TANKER

The specifications of the FPSO and shuttle tanker used in the present study are summarized in Table 1. The FPSO has 12 chain-polyester-chain mooring lines and 13 risers. There are four groups of lines, each group consists of 3 lines 5-degrees apart. Each mooring line has a studless chain anchor of Grade K4. The effects of tangential drag and tangential added inertia of mooring lines and friction damping from seabed were expected to be unimportant, and thus they were not included in this study. For simplify the analysis, four equivalent mooring lines and one equivalent riser were used in the simulation, with each equivalent line representing the combined effects of 3 mooring lines. The equivalent diameter was derived from the condition of equal drag and inertia force. Table 2 and 3 show the main particulars and hydrodynamic coefficient of mooring lines, riser and hawser.

Fig. 4 shows distribution of panels on FPSO and shuttle tanker. Fig. 5 shows mooring systems, hawser connection, and environmental directions.

Table 1 Main particulars of the turret-moored FPSO and shuttle tanker

Designation	Unit	FPSO and Shuttle Tanker
Length LPP	m	310.00
Breadth	m	47.17
Draft	m	18.90
Displacement	m^3	240869.00
Water Plane Area	m^2	13400.00
Center of Gravity (KG)	m	13.32
Radius of Gyration (Roll)	m	15.79
Radius of Gyration (Pitch)	m	115.03
Radius of Gyration (yaw)	m	116.13
Frontal Wind Area	m^2	1012.00
Side Wind Area	m^2	3772.00
Turret Center Line Behind FPP	m	63.55

Table 2 Main particulars and hydrodynamic coefficient of mooring systems

Designation	Unit	Segment 1 Chain	Segment 2 Wire	Segment 3 Chain
Pretension	kN	1.74E+03	1.74E+03	1.74E+03
Length	m	9.14E+02	1.13E+03	9.14E+02
Diameter	mm	8.17E+02	6.93E+02	8.17E+02
Dry Weight	kg/m	5.68E+02	5.16E+01	5.68E+02
Wet Weight	kg/m	4.94E+02	1.35E+01	4.94E+02
Stiffness	kN/m	2.37E+06	5.60E+05	2.37E+06
Inertia Coeff.	-	2.00	1.12	2.00
Drag Coeff.	-	2.45	1.20	2.45

Table 3 Main particulars and hydrodynamic coefficient of riser and hawser

Designation	Unit	Riser	Hawser
Pretension	kN	1.14E+05	8.00E+05
Length	m	1.81E+03	N/A
Diameter	mm	2.76E+03	N/A
Dry Weight	kg/m	2.56E+03	2.89E+01
Wet Weight	kg/m	1.31E+03	N/A
Stiffness	kN/m	1.69E+08	1.87E+06
Inertia Coeff.	-	1.00	N/A
Drag Coeff.	-	1.00	N/A

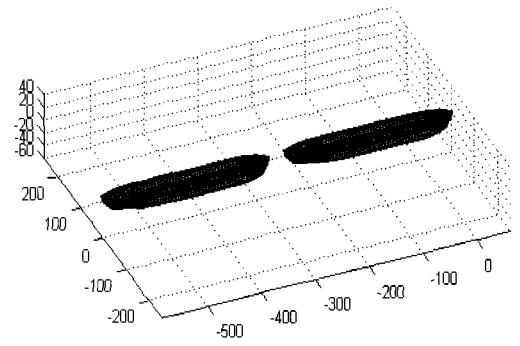

Fig. 4 Mash generation of tandem moored FPSO and shuttle tanker

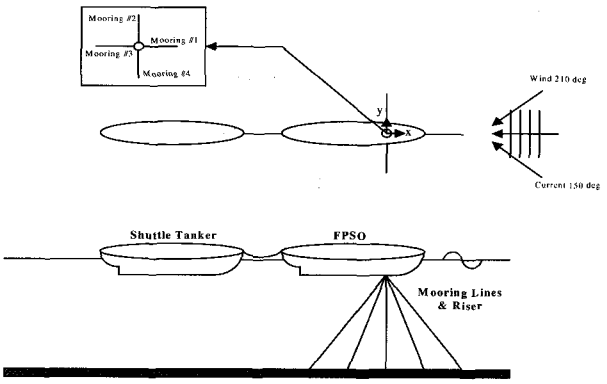

Fig. 5 Arrangement of mooring system, riser and hawser for tandem moored FPSO and shuttle

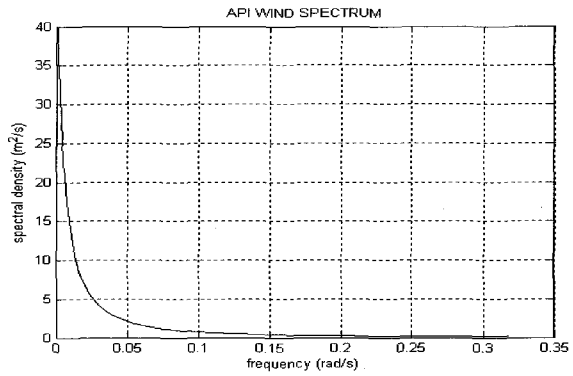

Fig. 6 API wind spectrum (at 10m above MWL, V_{10} = 5.0m/s)

4. DESCRIPTION OF CASE STUDY AND DESIGN ENVIRONMENTAL CONDITION

In this simulation, non-collinear West Africa environmental conditions are simulated. To simulate weathervane tandem moored floating bodies, the relative angle and distance between two bodies have to be considered to calculate hydrodynamic coefficients. To simplify the analysis, only relative angle between two bodies are considered for calculating hydrodynamic coefficients in WAMIT analysis. Table 4 summarize the environmental condition for tandem moored case. Fig. 6 illustrates the wind spectrum used in simulation.

The viscous force on FPSO and shuttle tanker is modeled by plate member and calculated by drag term in Morison equation. Wichers (1998, 2001a and 2001b) proposed hull drag coefficients. In the analysis, the hull viscous force in sway direction calculated by Wichers hull drag coefficient.

Table 4 Environmental condition for tandem moored FPSO and shuttle tanker (Non-collinear West African Sea)

	West African Sea		
Wave	Hs	(m)	2.70
(JONSWAP)	Tp	(sec)	16.50
	Gamma		6.00
	Direction	(deg)	180.00
Wind	V_{10}	(m/s)	5.00
(API Spectrum)	Direction	(deg)	210.00
Current	Free surface	(m/s)	0.15
(Steady)	at 60.96 m	(m/s)	0.15
	at 91.44 m	(m/s)	0.50
	Bottom	(m/s)	0.50
	Direction	(deg)	150.00

5. NUMERICAL SIMULATION RESULTS

To evaluate the hydrodynamic interaction effects between tandem moored FPSO and shuttle tanker, simulations are conducted by CMM and SMM. In the simulation, the distance between FPSO and shuttle tanker is 30m. During offloading operation, the tug boat control the distance between FPSO and shuttle tanker. In the simulation, the tug boat operation is simplified modeled as constant force (4.0E+05N) in surge direction of shuttle tanker. Fig. 7 shows the simulated wave time series and spectrum. The comparisons of the CMM and SMM are shown in Fig. 8 through 19, and Table 5 and 9. In tandem moored case, the hydrodynamic interactions between FPSO and shuttle tanker are relatively small compare to side by side moored case.

Thus, the CMM and SMM give almost identical results. Table 7 summarizes the difference of the motion statistics between CMM and SMM. Table 8 summarizes the relative motion statistic. The results show that the difference between two methods is almost negligible. The results also show that the off-diagonal 6×6 hydrodynamic interaction effects are not large on tandem moored case. Fig. 20, 21 and Table 9 show the mooring lines and hawser top tension spectra and statistics. Due to good agreement in the motion analysis results, the top tension on the mooring lines and hawser are almost identical in CMM and SMM. The results also show that the hawser can be solved by iteration method. It is interesting to notice that the slack side mooring line (mooring line # 3) has larger standard deviation than taut side mooring line. The reason is that minimum and maximum surge offset is small, thus low frequency components are comparable in taut and slack side, but the taut side mooring line (mooring #1) has small wave-frequency components compared to slack side mooring line (mooring #3). Thus, in this environment condition, the mooring line #3 experiences more dynamic tension than taut side mooring line (mooring line #1).

Table 5 Summary of motion statistics of tandem moored FPSO and shuttle tanker by CMM

		Combined Matrix Methods					
		Mean	Min	Max	STD	WF	LF
Surge	FPSO	-1.98E+00	-3.21E+00	-9.64E-01	3.68E-01	1.35E-01	3.63E-01
(m)	Shuttle	-2.00E+00	-4.42E+00	5.73E-01	9.25E-01	1.33E-01	9.18E-01
Sway	FPSO	3.97E-02	-8.62E-02	1.67E-01	4.71E-02	2.16E-03	4.72E-02
(m)	Shuttle	-4.64E+00	-8.07E+00	9.99E-02	2.37E+00	6.03E-02	2.37E+00
Heave	FPSO	-6.00E-01	-1.49E+00	3.58E-01	2.64E-01	2.64E-01	5.48E-03
(m)	Shuttle	7.76E-01	-1.90E+00	3.54E+00	8.75E-01	8.75E-01	2.91E-02
Roll	FPSO	8.35E-04	-1.23E-02	1.47E-02	2.83E-03	2.77E-03	5.79E-04
(deg)	Shuttle	9.05E-04	-1.43E-01	1.32E-01	3.07E-02	3.07E-02	2.54E-04
Pitch	FPSO	2.07E-01	-4.35E-01	9.13E-01	1.92E-01	1.92E-01	3.84E-03
(deg)	Shuttle	-2.68E-01	-1.36E+00	7.85E-01	3.47E-01	3.47E-01	1.1.5E-02
Yaw	FPSO	4.36E-01	-1.18E-01	9.58E-01	3.19E-01	0.00E+00	3.19E-01
(deg)	Shuttle	2.82E+00	2.33E-01	4.20E+00	9.93E-01	4.09E-02	9.92E-01

Table 6 Summary of motion statistics of tandem moored FPSO and shuttle tanker by SM

		Separate Matrix Methods					
		Mean	Min	Max	STD	WF	LF
Surge	FPSO	-1.98E+00	-3.19E+00	-9.36E-01	3.84E-01	1.28E-01	3.63E-01
(m)	Shuttle	-2.00E+00	-4.38E+00	5.26E-01	9.20E-01	1.26E-01	9.15E-01
Sway	FPSO	3.98E-02	-7.20E-02	1.60E-01	4.50E-02	7.17E-04	4.52E-02
(m)	Shuttle	-4.53E+00	-7.98E+00	1.00E-01	2.52E+00	6.44E-02	2.52E+00
Heave	FPSO	-6.00E-01	-1.50E+00	3.37E-01	2.65E-01	2.64E-01	5.88E-03
(m)	Shuttle	7.76E-01	-1.86E+00	3.49E+00	8.55E-01	8.54E-01	2.74E-02
Roll	FPSO	8.32E-04	-7.03E-03	1.09E-02	2.41E-03	2.35E-03	5.63E-04
(deg)	Shuttle	9.18E-04	-1.30E-01	1.30E-01	3.39E-02	3.39E-02	2.44E-04
Pitch	FPSO	2.07E-01	-4.61E-01	9.18E-01	1.93E-01	1.93E-01	2.16E-03
(deg)	Shuttle	-2.68E-01	-1.34E+00	7.67E-01	3.39E-01	3.39E-01	1.08E-02
Yaw	FPSO	4.18E-01	-1.44E-01	9.55E-01	3.40E-01	0.00E+00	3.40E-01
(deg)	Shuttle	2.79E+00	2.33E-01	4.23E+00	1.01E+00	4.37E-02	1.01E-01

Table 7 Motion difference between CMM and SMM

		Difference					
		Mean	Min	Max	STD	WF	LF
Surge (m)	FPSO	1.094E-04	-1.74E-02	-2.76E-02	2.40E-03	6.81E-03	4.06E-05
	Shuttle	1.87E-03	-4.10E-02	4.68E-02	4.48E-03	6.85E-03	3.57E-03
Sway (m)	FPSO	-3.62E-05	-1.42E-02	6.79E-03	6.79E-03	1.45E-03	2.06E-03
	Shuttle	-1.08E-01	-9.68E-02	-3.26E-04	-3.26E-04	-4.12E-03	-1.53E-01
Heave (m)	FPSO	-6.49E-05	6.70E-03	2.05E-02	2.05E-02	-9.37E-04	-3.93E-04
	Shuttle	1.41E-04	-4.41E-02	4.45E-02	4.45E-02	2.07E-02	1.76E-03
Roll (deg)	FPSO	3.49E-06	-5.27E-03	3.76E-03	3.76E-03	4.27E-04	1.70E-05
	Shuttle	-1.27E-05	-1.28E-02	1.86E-03	1.86E-03	-3.24E-03	1.00E-05
Pitch (deg)	FPSO	-9.13E-05	2.63E-02	-5.29E-03	-5.29E-03	-8.51E-04	1.68E-03
	Shuttle	-5.34E-05	-1.81E-02	1.79E-02	1.79E-02	8.26E-03	6.73E-04
Yaw (deg)	FPSO	1.74E-02	2.63E-02	3.53E-03	3.53E-03	0.00E+00	-2.08E-02
	Shuttle	2.51E-02	-1.11E-04	-3.36E-02	-3.36E-02	-2.79E-03	-1.80E-02

Table 8 Summary of relative motion statistics of tandem moored FPSO and shuttle tanker

		Surge (m)	Sway (m)	Heave (m)
CMM	MAX	2.13E+00	8.09E+00	1.71E+00
	MIN	-2.22E+00	-6.70E-02	-4.10E+00
	STD	8.71E-01	2.36E+00	9.28E-01
SMM	MAX	2.10E+00	7.98E+00	1.59E+00
	MIN	-2.15E+00	-6.83E-02	-4.02E+00
	STD	8.65E-01	2.52E+00	8.96E-01

Table 9 Summary of tension statistics

	Mooring #1		Mooring #3		Hawser	
	CMM	SMM	CMM	SMM	CMM	SMM
Mean (N)	4.49E+06	4.49E+06	3.90E+06	3.90E+06	5.18E+05	5.18E+05
Min (N)	4.32E+06	4.33E+06	3.64E+06	3.64E+06	4.23E+05	4.25E+05
Max (N)	4.65E+06	4.65E+06	4.17E+06	4.16E+06	6.11E+05	6.10E+05
STD (N)	5.85E+04	5.79E+04	7.73E+04	7.71E+04	3.79E+04	3.75E+04

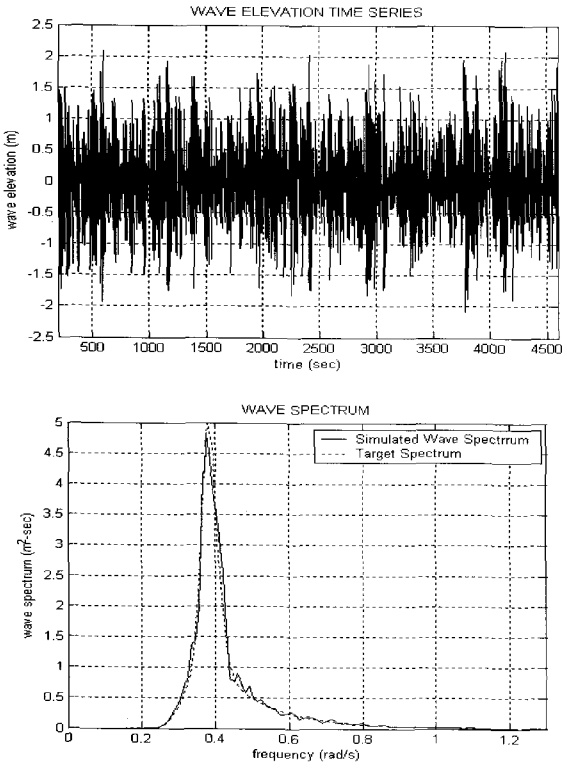

Fig. 7 Wave time series and spectrum (West African Sea)

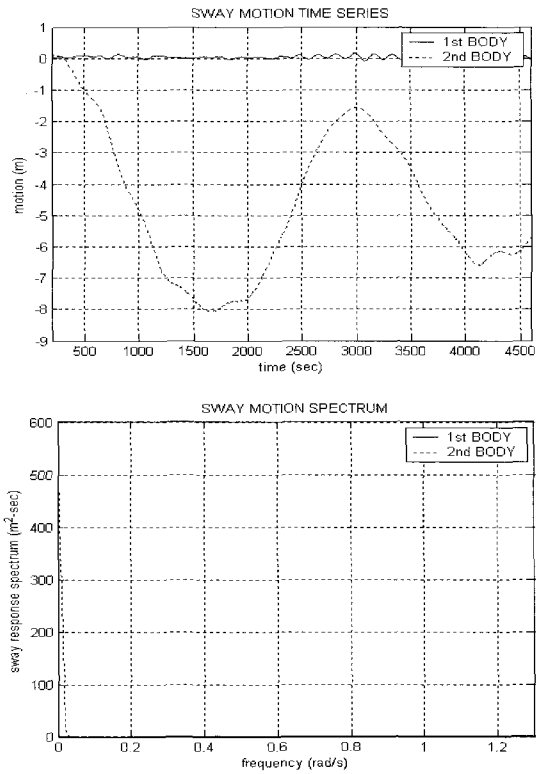

Fig. 9 Sway motion time series and spectrum by CMM

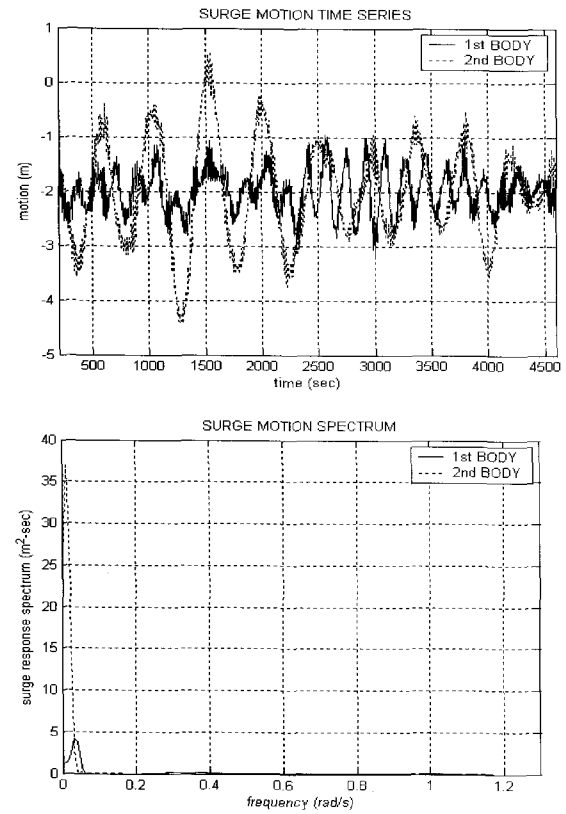

Fig. 8 Surge motion time series and spectrum by CMM

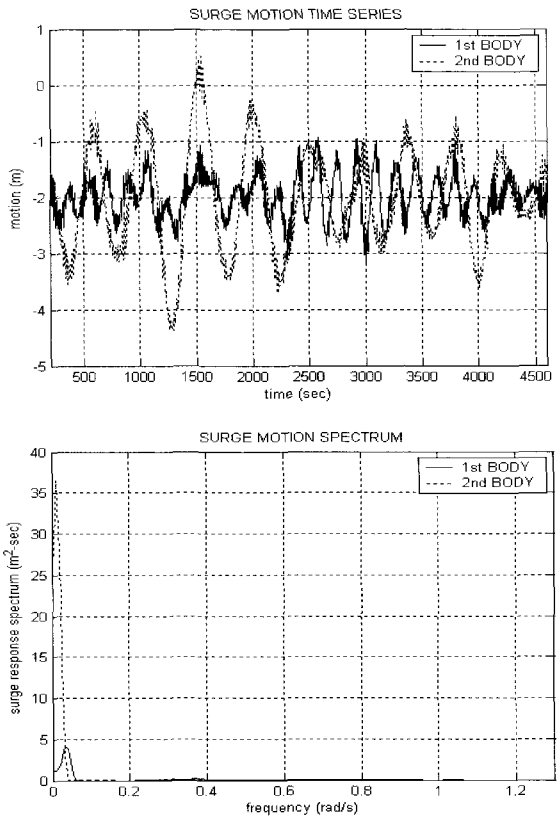

Fig. 10 Surge motion time series and spectrum by SMM

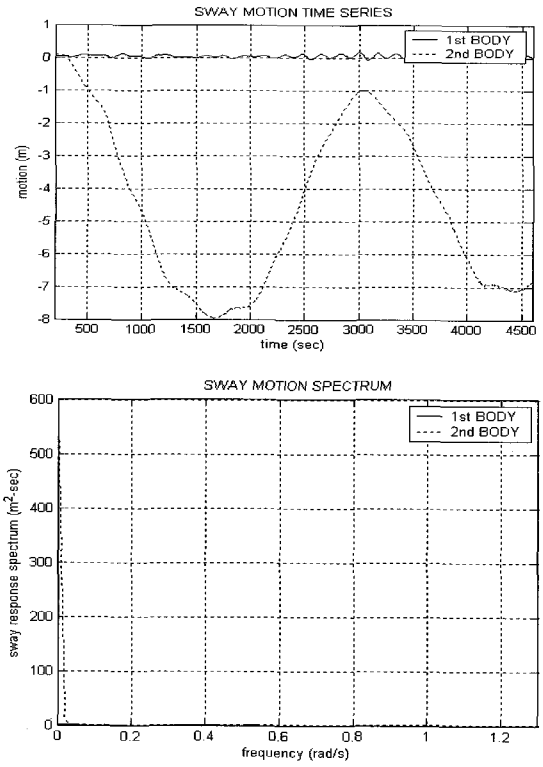

Fig. 11 Sway motion time series and spectrum by SMM

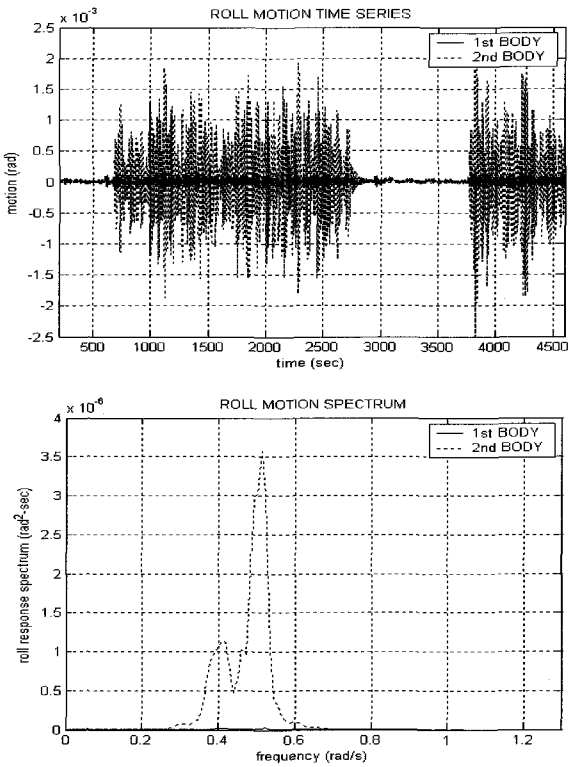

Fig. 13 Roll motion time series and spectrum by CMM

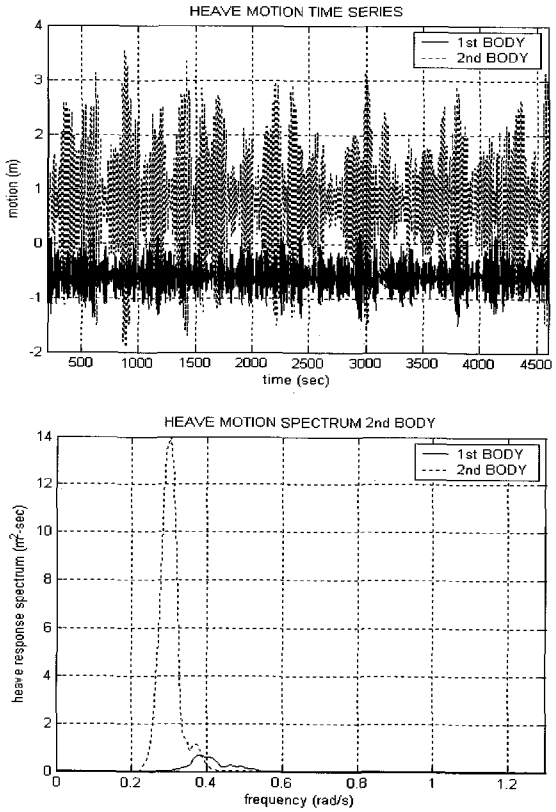

Fig. 12 Heave motion time series and spectrum by CMM

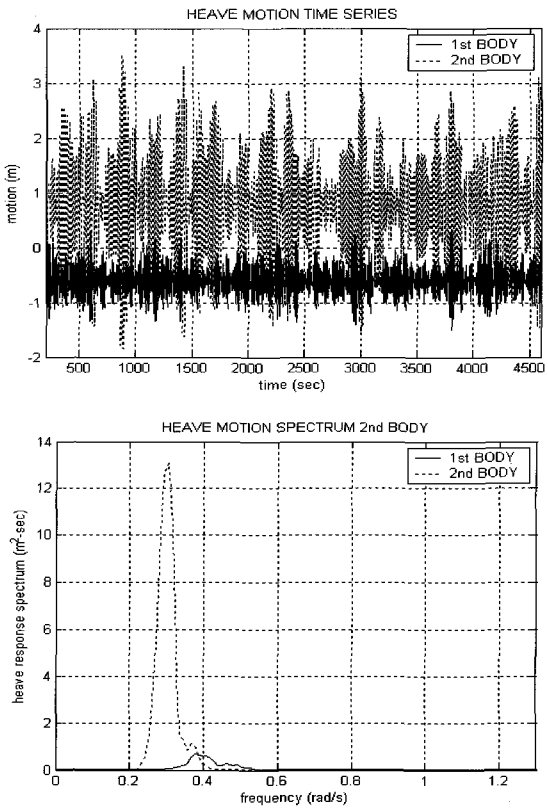

Fig. 14 Heave motion time series and spectrum by SMM

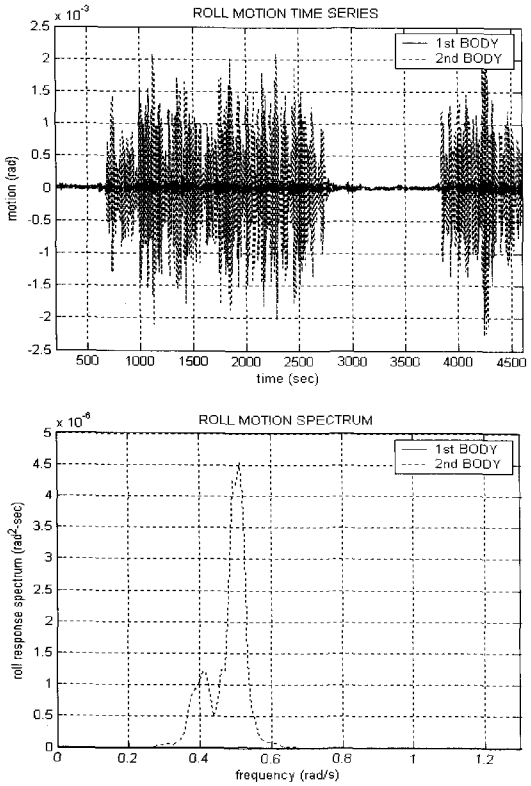

Fig. 15 Roll motion time series and spectrum by SMM

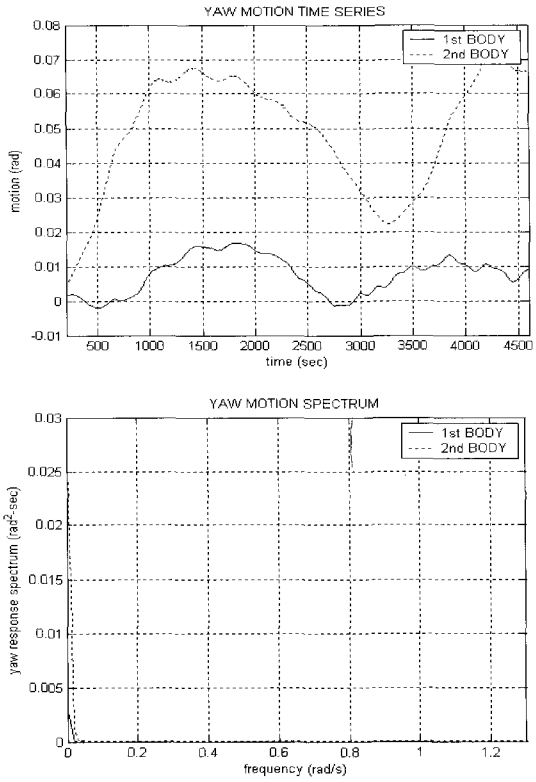

Fig. 17 Yaw motion time series and spectrum by CMM

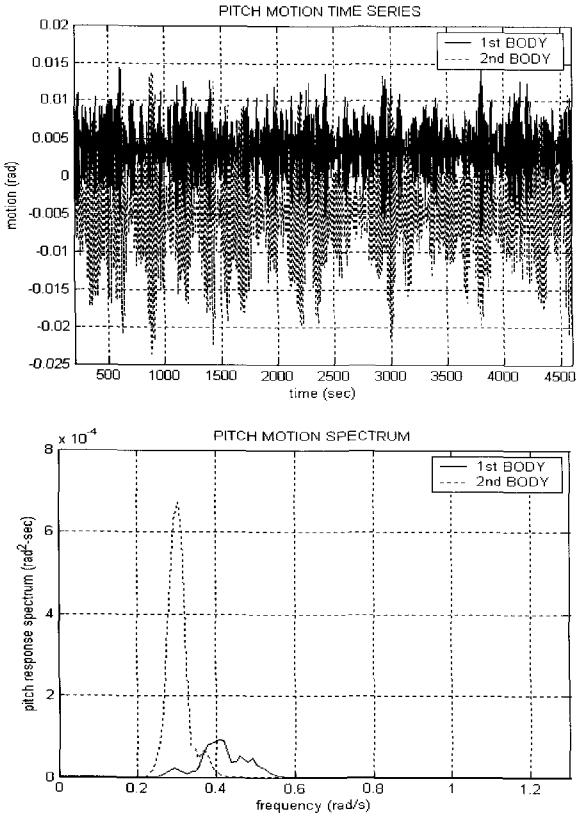

Fig. 16 Pitch motion time series and spectrum by CMM

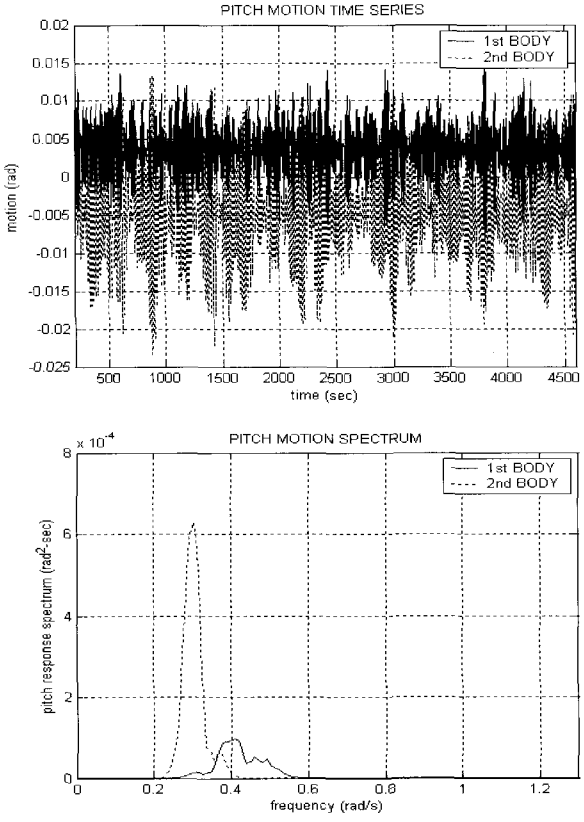

Fig. 18 Pitch motion time series and spectrum by SMM

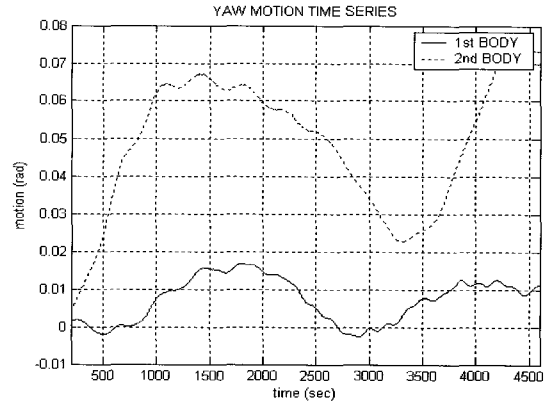

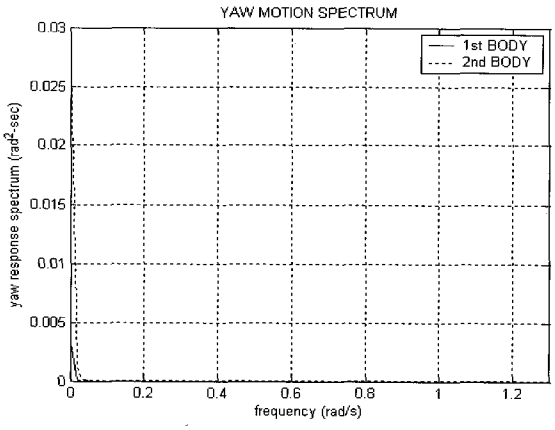

Fig. 19 Yaw motion time series and spectrum by SMM

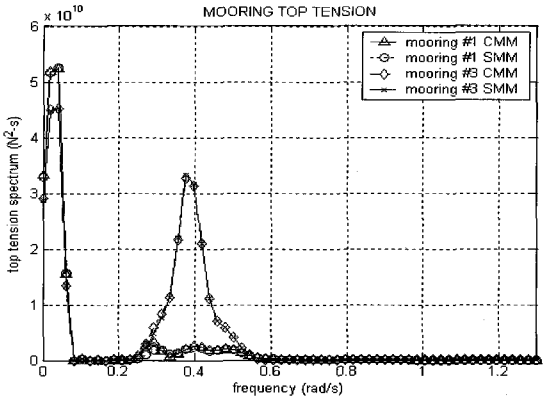

Fig. 20 Top tension spectra of mooring lines

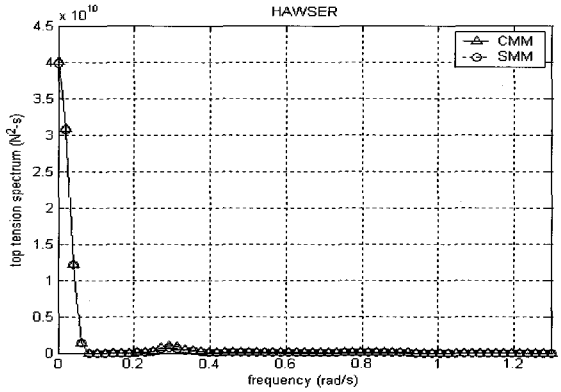

Fig. 21 Tension spectra of hawser

6. CONCLUSION

The operability of multiple floating bodies offloading operation greatly influenced by arrangement of vessels and relative motions among vessels. Therefore, the accurate motion prediction of vessels including hydrodynamic interactions with elastic lines (i.e. hawser, mooring, and riser) is greate importance. Motion analysis of multiple floating bodies connected by numerous lines can be analyzed by three typical methods. The first method is iteration method between two vessels without considering hydrodynamic interaction effects. The second method (CMM) is exact time domain methods including all the 12N×12N hydrodynamic interaction effects and line dynamics effects.

The third method (SMM) is time domain iteration method between two vessels considering direct hydrodynamic interaction effects (i.e. includes 6×6 direct interaction terms and ignore 6×6 cross coupling terms) and line dynamic effects. The simulation results show that, in tandem moored case, Separated Matrix Method (SMM) and Combined Matrix Method (CMM) give good agreement.

For side by side moored case, the hydrodynamic interaction effects are expected to be large. However, in tandem moored case, the distance between floating bodies (i.e. 30m) is large enough to reduce large hydrodynamic interaction, and the tandem moored arrangement of the two vessels is also reduce hydrodynamic interaction. Due to this reason, in tandem moored case, the Separated Matrix Method (SMM), which is partially consider hydrodynamic interaction effects and fully consider mechanical coupling effects, gives almost identical results compare with Combined Matrix Method (CMM). Therefore, to save calculation time, Separated Matrix Method (SMM) is more efficient than Combined Matrix Method (CMM) in tandem moored arrangement.

REFERENCE

Arcandra, T. (2001), "Hull/Mooring/Riser Coupled Dynamic Analysis of a Deepwater Floating Platform with Polyester Lines", Ph.D. Dissertation, Civil Engineering Department, Texas A&M University, College Station, TX.

Arcandra, T., Nurtjahyo, P. and Kim, M.H., (2002), "Hull/Mooring/Riser Coupled Analysis of a Turret-Moored FPSO 6000 ft: Comparison between Polyester and Buoys-Steel Mooring Lines", Proc. 11th Offshore Symposium The Texas Section of the Society of Naval Architects and Marine Engineers, SNAME, pp 1-8.

Buchner, B., Dijk, A. and Wilde, J. (2001), "Numerical Multiple-Body Simulations of Side-by-Side Mooring To a n FPSO", Proc. 11th Int. Offshore and Polar Eng. Conference, ISOPE, Vol 1, pp 343-353.

Choi, Y.R. and Hong, S.Y. (2002), "An Analysis of Hydrodynamic Interaction of Floating Multi-Body Using Higher-Order Boundary Element Method" Proc. 12th Int. Offshore and Polar Eng. Conference, ISOPE, Vol 1, pp 303-308.

Fang, M.C. and Kim, C.H. (1986), "Hydrodynamically Coupled Motions of Two Ship Advancing in Oblique Waves", Journal of Ship Research, Vol 30 (3), pp 159-171.

Garrett, D.L. (1982), "Dynamic Analysis of Slender Rods" Journal Energy Resources Technology, Vol 104, pp 302-307.

Hong, S.Y., Kim, J.H., Cho, S.K., Choi, Y.R., and Kim, Y.S. (2003), "Numerical and Experimental Study on Hydrodynamic Interaction of Side-by-Side Moored Multiple Vessels", Proc. of Deep Water Mooring System, ASCE, pp 198-215.

Kim, M.H., Arcandra, T. & Kim, Y.B., (2001a), "Validability of Spar Motion Analysis against Various Design Methodologies/Parameters", Proc. 20th Offshore Mechanics and Arctic Eng. Conference, OMAE01-OFT1063 [CD-ROM], L.A., Califonia.

Kim, M.H., Arcandra, T. and Kim, Y.B. (2001b), "Validability of TLP Motion Analysis against Various Design Methodologies/Parameters" Proc. 11th Int. Offshore and Polar Eng. Conference, ISOPE, Vol 3, pp 465-473.

Kim, Y.B. (2003) "Dynamic Analysis of Multiple-Body Floating Platforms Coupled with Mooring Lines and Risers", Ph.D. Dissertation, Civil Engineering Department, Texas A&M University, College Station,

Kodan, N. (1984), "The Motion of Adjacent Floating Structure in Oblique Waves". Proc. 3rd Offshore Mechanics and Arctic Eng. Conference, OMAE, New Orleans, Vol 1, pp 206-213.

Koo, B.J., Kim M.H., and Randall, R.E. (2004), "The Effect of Nonlinear Multi-contact Coupling with Gap between Risers and Guide Frames on Global Spar Motion Analysis", J. of Ocean Engineering. Vol 31/11-12, pp 1469-1502.

Lee D.H. (2002) "Nonlinear Stability Analysis and Motion Control of Tandem Moored Tankers", Ph.D. Dissertation, Naval Architecture and Ocean Engineering, Seoul National University.

Lee, C.H. (1999), WAMIT Theory Manual. Department of Ocean Engineering. MIT.

Lee, D.H. and Choi, H.S. (2000), "A Dynamic Analysis of FPSO-Shuttle Tanker System", Proc. 10th Int. Offshore and Polar Eng. Conference, ISOPE, Vol 1, pp 302-307.

Loken A.E. (1981), "Hydrodynamic Interaction between Several Floating Bodies of Arbitrary form in Waves. Proc. of Intl Symposium on Hydrodynamics in Ocean Engineering", NIT, Trondhiem, Vol 2, pp 745-779.

Ma, W., Lee, M.Y., Zou, J., and Huang, E.W. (2000), "Deepwater Nonlinear Coupled Analysis Tool", Offshore Technology Conference, (OTC 12085), Houston, TX.

Ohkush, M. (1974), "Ship Motions in Vicinity of a Structure" Proc. of Intl Conf. on Behavior of Offshore Structure, NIT, Trondheim, Vol 1, pp 284-306.

Sphaier, S.H., Fernandes, A.C., and Correa, S.H. (2000), "Maneuvering model for the FPSO horizontal plane behavior", Proc. 10th Int. Offshore and Polar Eng. Conference, Vol 1, pp 337-344.

Van Oortmerssen, G. (1979), "Hydrodynamic Interaction between Two Structures of Floating in Waves" Proc. Boss 79. 2nd Intl Conf. on Behavior of Offshore Structure, London, pp 339-356.

Wichers, J.E. W., Voogt, H.J., Roelofs, H.W. and Driessen, P.C.M. (2001b), "DeepStar-CTR 4401- Benchmark Model Test. Technical", Rep. No 16417-1-OB, MARIN, Wageningen, Netherlands.

Wichers, J.E.W. and Develin, P.V. (2001a), "Effect of Coupling of Mooring Lines and Risers on the Design Values for a Turret Moored FPSO in Deep Water of the Gulf of Mexico", Proc. 11th Int. Offshore and Polar Eng. Conference, 3, pp 480-487.

Wichers, J.E.W. (1988), "A Simulation Model for a Single Point Moored Tanker", Ph.D. Dissertation, Delft University of Technology, Delft, The Netherlands.

2005년 7월 12일 원고 접수
2005년 10월 13일 최종 수정본 채택